

Study of ZnO Nanospheres Fabricated via Thermal Evaporation for Solar Cell Application

Fatin Farisha Alia Azmi¹, Bouchta Sahraoui², and Saifful Kamaluddin Muzakir^{1*}

1. Material Technology Programme, Faculty of Industrial Sciences & Technology, Universiti Malaysia Pahang, Lebuhraya Tun Razak, Gambang 26300, Kuantan, Pahang, Malaysia
2. University of Angers, UFR Sciences, Institute of Sciences and Molecular Technologies of Angers MOLTECH Anjou-UMR CNRS 6200, 2 Bd Lavoisier 49045 ANGERS cedex 2, France

*e-mail: saifful@ump.edu.my

Abstract

A solar cell is a device that absorbs light energy to generate electrical energy. A typical example of a solar cell is the quantum dot solar cell (QDSC), which consists of three main components: (i) fluorophore: the component that absorbs light and generates excited state electrons and holes, (ii) photoelectrode: the component that transports the excited state electron and prevents recombination of excited state electrons and holes, and (iii) electrolyte: the component that replenishes the vacancy left by the excited electron in the hole. Despite the increasing number of research in the QDSC field, to date, a device with significant photovoltaic efficiency has not been developed. In this study, the mechanism of electron transport in a zinc oxide (ZnO) photoelectrode was investigated. Two ZnO layers were fabricated using thermal evaporation method at different vacuum pressures (5×10^{-4} and 5×10^{-5} Torr). Two solar cells were fabricated using ZnO as photoelectrode, lead sulphide as fluorophore, and a mixture of carboxymethyl cellulose and polyvinyl alcohol as electrolyte. The cell which utilized the ZnO fabricated under 5×10^{-5} Torr showed the highest efficiency ($\eta = 0.98\%$), with fill factor = 22.07%, short circuit current = 2.85 mA/m², and open circuit voltage = 80.719 mV.

Abstract

Kajian Tentang Bola-Bola Nano ZnO Yang Dibuat Melalui Penguapan Termal untuk Penerapan Sel Surya. Suatu sel surya merupakan suatu alat yang menyerap energi cahaya untuk membangkitkan energi listrik. Contoh yang khas dari suatu sel surya adalah sel surya titik kuantum (quantum dot solar cell (QDSC)), yang terdiri atas tiga komponen utama: (i) fluorofofor (zat pendar fluor): komponen yang menyerap cahaya dan membangkitkan elektron dan rongga dalam keadaan tereksitasi, (ii) fotoelektroda (elktroda cahaya): komponen yang mengangkut elektron-elektron dalam keadaan tereksitasi dan mencegah penggabungan kembali elektron-elektron tereksitasi dengan rongga-rongga, and (iii) elektrolit: komponen yang mengisi kembali tempat kosong yang ditinggalkan oleh elektron yang tereksitasi di dalam rongga tadi. Sekalipun jumlah riset di bidang QDSC terus bertambah, hingga kini, belum dikembangkan suatu alat dengan efisiensi fotovoltaiik yang signifikan. Di dalam kajian ini, diteliti mekanisme pengangkutan elektron di dalam suatu fotoelektroda zink oksida (ZnO). Dua lapisan ZnO dibuat dengan menggunakan metode penguapan panas pada tekanan vakum yang berbeda (5×10^{-4} dan 5×10^{-5} Torr). Dua buah sel surya dibuat dengan menggunakan ZnO sebagai fotoelektroda, timbal sulfida sebagai fluorofofor, dan suatu campuran karboksimetil selulosa dan polivinil alkohol sebagai elektrolit. Sel yang menggunakan ZnO yang dibuat pada tekanan 5×10^{-5} Torr menunjukkan efisiensi tertinggi ($\eta = 0.98\%$), dengan faktor pengisi = 22,07%, arus hubungan pendek = 2,85 mA/m², dan tegangan sirkuit terbuka = 80,719 mV.

Keywords: efficiency, fluorophore, thermal evaporation, photoelectrode, zinc oxide

1. Introduction

Quantum dot solar cells (QDSCs) have attracted extensive interest because of their maximum theoretical efficiency, which exceeds 60% [1], and low-cost materials [2]. Their maximum theoretical efficiency exceeds that of

their analogue, dye sensitized solar cells (DSSCs), by ~30% because of the multiple exciton generation in the quantum dots [3], [4]. The archetypical QDSC device structure of ZnO/PbS has recorded the highest efficiency (~6.59%) and showed outstanding atmospheric stability [5–7].

Solar cells photoelectrodes attract less attention, although they play an important role in solar cells. Titanium dioxide (TiO₂) is a commonly used photoelectrode that has attracted attention from researchers worldwide [8]; however, ZnO offers an alternative to TiO₂ because of its high electron mobility and great diversity of synthesizable morphologies, e.g., nanoparticles, nanorods, and nanosheets. Moreover, ZnO has a direct wide bandgap of 3.37 eV and large exciton binding energy of 60 meV [9].

Zinc oxide layers have been fabricated by various techniques [10], such as thermal evaporation [11–15], pulsed laser deposition [16], sol-gel [17, 18], and chemical vapor deposition [19, 20]. Among these, thermal evaporation is an attractive technique because of multi-layer fabrication, thickness controllability [21], and high deposition rates [22].

Nevertheless, it is very challenging to synthesize ZnO in a quantum-confined region (smaller than the exciton Bohr radius of ZnO, ~1.8 nm) directly onto the surface of substrates. However, the thermal evaporation method offers controllable parameters (temperature, vacuum pressure, voltage, and current) to fine-tune the morphology and size of the yield. In this study, the effect of different vacuum pressure environments toward the morphology and optical properties of the yielded ZnO was investigated.

2. Methods

Materials. Zinc oxide (Aldrich, 99.9%), lead (II) sulfide (Aldrich, 99.9%), and carboxymethyl cellulose and polyvinyl alcohol (CMC/PVA, 80:20 composition) were used in this study.

Device Fabrication. Thin films of fluorophore (PbS) and photoelectrode (ZnO) were fabricated using thermal evaporation; these films acted as the working electrodes of a solar cell. An indium-doped tin oxide (ITO) conducting glass (100 mm × 100 mm × 1.1 mm) was cut into 2.5 cm × 2.5 cm. A ZnO thin film was fabricated onto the ITO with an active area of 1 cm × 1 cm.

Zinc oxide powder (0.16274 g) was thermally evaporated and successfully fabricated on the ITO under three conditions: (i) pressure of 1.5×10^{-3} Torr, voltage of 1.52 V, and current of 63 A; (ii) 5×10^{-4} Torr, 1.59 V, and 72 A; and (iii) 5×10^{-5} Torr, 2.6 V, and 116 A. After fabricating the ZnO layer, a PbS (0.24 g) layer was fabricated on the surface of the ZnO layer using similar procedure, at 1.5×10^{-3} Torr, 1.53 V, and 65 A.

A polymer-based electrolyte was prepared by dissolving 2 g of CMC/PVA mixture (80:20 by weight) in 100 ml of distilled water. The mixture was continuously stirred for ca. 24 hours to form a homogenous solution. The prepared polymer-based electrolyte was then

sandwiched in between the working electrode and a counter electrode (blank ITO).

A field-emission scanning electron microscope (JSM-7800F Schottky), X-ray diffractometer (Rigaku Miniflex II), and ultraviolet-visible spectrophotometer (Shimadzu UV-2600) were individually used to characterize the morphology, crystal structure, and optoelectronic properties of the ZnO thin film. Then, the generated cells were characterized using a potentiostat-galvanostat.

3. Results and Discussion

Structural characterization. The crystal structures of the ZnO and ZnO/PbS layers were studied using X-ray diffraction (XRD), with diffraction angle of 10°–80° (Figure 1). In sample A (bare ZnO), peaks corresponding to ZnO were identified at angles 36.45°, 39.13°, and 43.33°, which agrees well with previous works [23]; the peaks were indexed to (002), (100), and (101) crystal planes of hexagonal wurtzite structure. However, the existence of high intensity peaks at 39.13° and 43.60° (marked with “x”), which correspond to zinc, indicates that the parameters (i.e., 1.5×10^{-3} Torr, 1.52 V, and 63 A) need to be fine-tuned, which would yield zinc oxide layer without contamination of excess zinc.

The zinc peaks disappeared (Figure 1b and 1c) upon optimization of the parameters during the fabrication of ZnO/PbS layers. Two sets of parameters were used for the ZnO/PbS fabrication: sample B (5×10^{-4} Torr, 1.59 V, and 72 A) and sample C (5×10^{-5} Torr, 2.60 V, and 116 A). Characteristic diffraction peaks of PbS at angles of 30.23°, 35.24°, 50.48°, 60.27°, and 64.15° corresponding to (111), (200), (220), (311), and (222) crystal planes, respectively, confirmed the presence of a PbS layer [24].

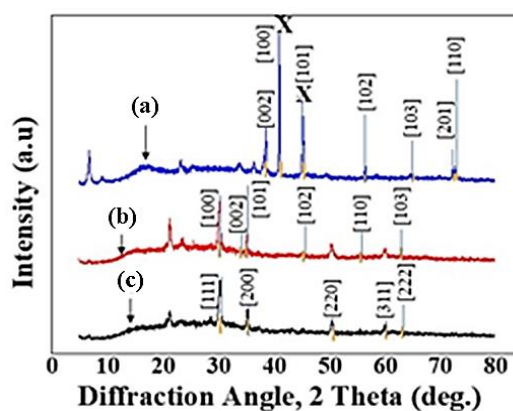


Figure 1. XRD Patterns of (a) Bare ZnO, (b) ZnO/PbS at 5×10^{-4} Torr, and (c) ZnO/PbS at 5×10^{-5} Torr. The Peaks Marked with “x” Correspond to Excess Zinc during the Fabrication

The morphology of the yielded ZnO (spherical) fabricated via thermal evaporation technique was modeled based on the XRD data using SHAPE V7 software package (Figure 2a). The fabricated ZnO layers were analyzed using field-emission scanning electron microscopy (FESEM), which revealed the nanosphere morphology had a size of 10–25 nm (Figure 2b).

Optical characterization. Absorption spectra of ZnO (sample A), ZnO/PbS thin films (samples B and C), and bare PbS (inset) are shown in Figure 3. Bare ZnO showed two absorption peaks, at 347 nm and 532 nm, similar to the reported literature value [25]. Upon careful excitonic peak fitting, the bare PbS showed three absorption peaks at 355 nm, 503 nm, and 661 nm, as the first, second, and third excitonic peaks, respectively.

A small redshift of the peaks was observed upon sensitization of the bare ZnO using PbS (Figure 3b and c), i.e., ca. 353 nm and 561 nm, which indicates a successful sensitization procedure.

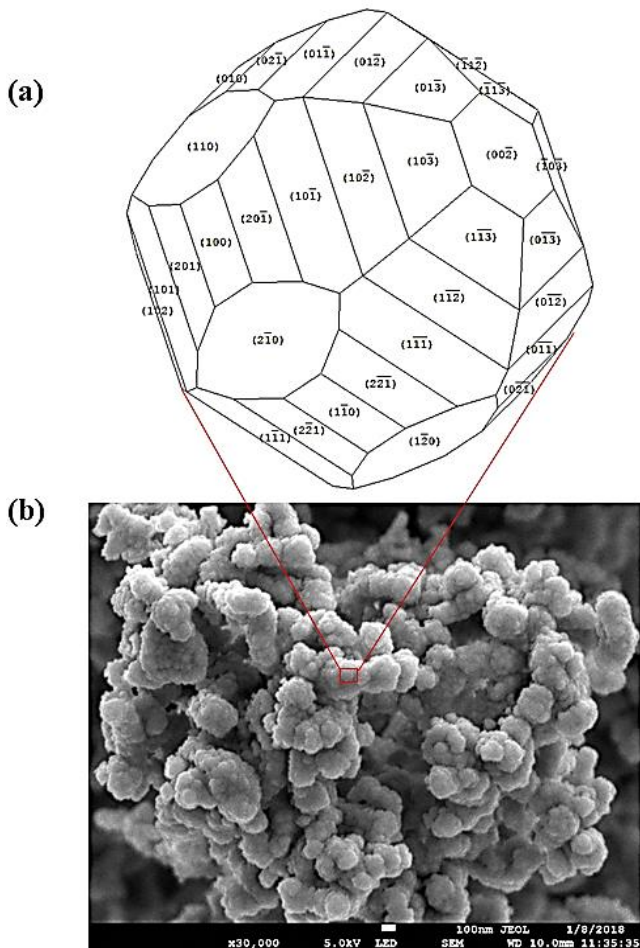


Figure 2. (a) Morphology of ZnO nanosphere modeled using SHAPE V7 software package and (b) nanosphere morphology revealed using FESEM

The sensitization mechanism of PbS was further analyzed using Tauc's plot (Figure 4) by comparing the bandgap (E_g) of the bare ZnO, bare PbS, and ZnO/PbS layers. The E_g was calculated using the following equations [26, 27]:

$$\alpha = \frac{1}{t} \left(\frac{A}{\log e} \right) \quad (1)$$

$$ahv = A(hv - E_g)^{1/2} \quad (2)$$

where t is the thickness of quartz cell, A is the absorbance of the samples, e is the charge of an electron, h is Planck constant, ahv is the energy of photon, and E_g is the bandgap [28].

The E_g of bare ZnO and bare PbS were estimated as 2.31 eV and 2.18 eV, respectively. The E_g of ZnO/PbS with ZnO layers fabricated at 5×10^{-4} Torr and 5×10^{-5} Torr were estimated as ca. 2.58 eV and 2.80 eV, respectively. The E_g of the ZnO/PbS conjugate was observed to be wider than that of the bare PbS, which indicates a successful sensitization of the ZnO using PbS.

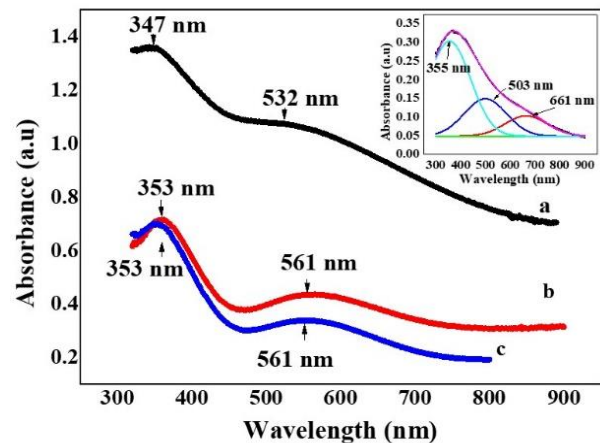


Figure 3. Absorption Spectra of (a) Bare ZnO with Absorption Peaks at 347 nm and 532 nm, (b) ZnO/PbS (Fabricated at 5×10^{-4} Torr) with Absorption Peaks at 353 nm and 561 nm, (c) ZnO/PbS (Fabricated at 5×10^{-5} Torr) with Absorption Peaks at 353 nm and 561 nm. Inset shows the Fitting of the First, Second, and Third Excitonic Peaks of Bare PbS (643 nm, 551 nm, and 458 nm, Respectively)

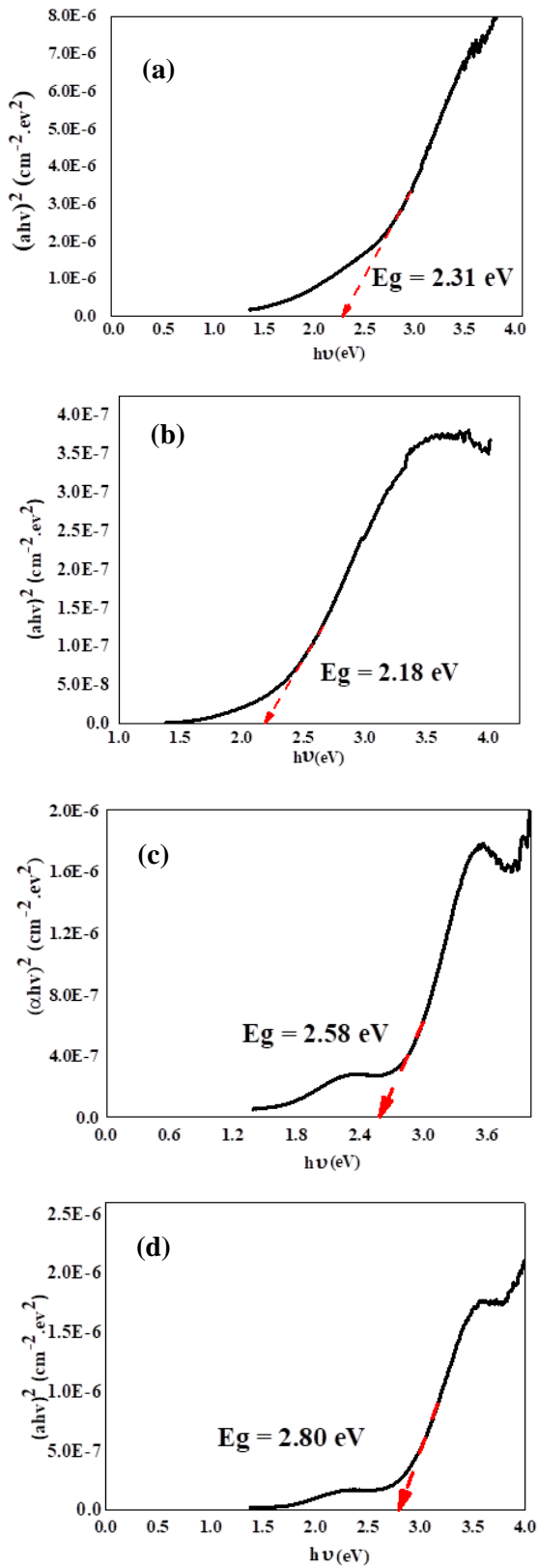


Figure 4. Tauc's Plot of (a) Bare ZnO at 1.5×10^{-3} Torr, (b) Bare PbS at 1.5×10^{-3} Torr, (c) ZnO/PbS at 5×10^{-4} Torr, and (d) ZnO/PbS at 5×10^{-5} Torr

Photovoltaic studies. The polymeric electrolyte was sandwiched between the working and counter electrodes. The current-voltage (I - V) measurements of the completed cells were carried out at 1000 W/m^2 of illumination.

The photovoltaic conversion efficiencies obtained for the PbS/ZnO-based cells fabricated at different pressures are summarized in Figure 5. The photovoltaic parameters (V_{OC} , I_{SC} , FF , η) were calculated using equations established elsewhere [29].

The poor η of both cells, i.e., 0.99% and 0.00181%, may be due to the poor quality of fabrication method, which can be observed from the low FF , i.e., 22.07% and 5.91%, respectively. The open circuit voltage (V_{OC}) of the cell corresponds to the difference between the redox potential of the electrolyte and the energy level of the highest occupied molecular orbital (HOMO) of the ZnO. Moreover, V_{OC} reduction was observed for the cell with ZnO fabricated at 5×10^{-5} Torr of pressure. This may be due to the small size of ZnO nanospheres fabricated at low pressure (5×10^{-5} Torr) compared to that fabricated at high pressure (5×10^{-4} Torr).

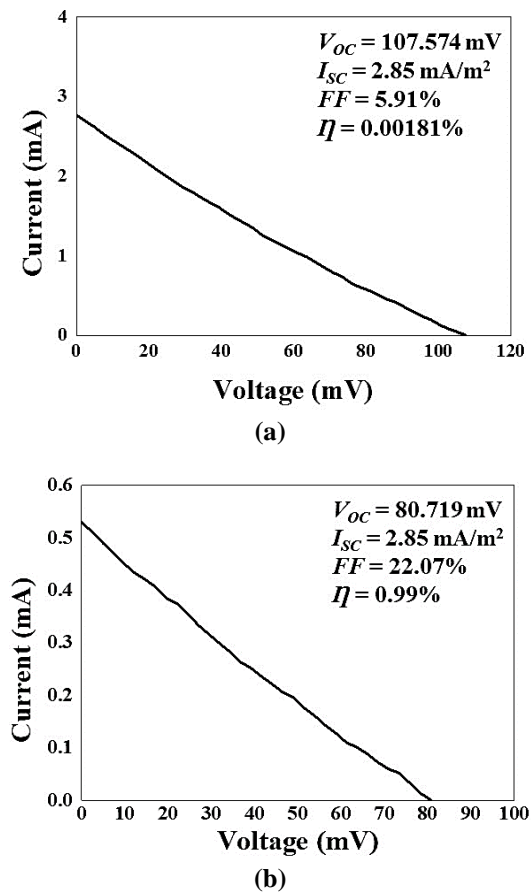


Figure 5. I - V Curve of the Cells Employing ZnO Fabricated at (a) 5×10^{-4} Torr and (b) 5×10^{-5} Torr

The ZnO nanocrystals characterized by size reduction toward their exciton Bohr radius (~1.8 nm) will present peculiar optoelectronic properties, i.e., E_g expansion according to the increment or decrement of the HOMO and the lowest unoccupied molecular orbital energy levels. This observation agrees well with the E_g analysis (in the previous section) in which the ZnO/PbS conjugate fabricated at low pressure presented a higher E_g than that fabricated at high pressure.

However, both cells surprisingly presented the same short circuit current (I_{SC} ~2.85 mA/m²); this may be because similar amount of PbS was adsorbed on the ZnO surface. Therefore, the ZnO fabricated at low and high pressures may have similar specific surface areas, despite the size difference.

4. Conclusions

Using the thermal evaporation technique, ZnO nanospheres were successfully fabricated under different conditions. The fabrication pressure, voltage, and current are important parameters that affect the size of the yield. Furthermore, the type of reactants can also be optimized to yield various morphologies and sizes of ZnO.

Acknowledgements

The author acknowledges the contribution of Universiti Malaysia Pahang through the research grant RDU 150111 for this work.

References

- [1] D.R. Baker, P.V. Kamat, *Adv. Funct. Mater.* 19 (2009) 805.
- [2] J. Tian, G. Cao, *J. Phys. Chem. Lett.* 6 (2015) 1859
- [3] M. Wang, C. Huang, Y. Cao, Q. Yu, Z. Deng, Y. Liu, J. Liang, *J. Phys. D* 42 (2009) 155104.
- [4] R.A. Ze'ev, M. Gharghi, A. Niv, C. Gladden, X. Zhang, *Sol. Energ. Mater. Sol. Cells.* 99 (2012) 308.
- [5] X. Lan, O. Voznyy, A. Kiani, F.P. García de Arquer, S.A. Abbas, G.H. Kim, M. Yuan, *Adv. Mater.* 28 (2016) 299.
- [6] M. Liu, F.P.G. de Arquer, Y. Li, X. Lan, G.H. Kim, O. Voznyy, J.Y. Kim, *Adv. Mater.* 28 (2016) 4142.
- [7] C.H.M. Chuang, P.R. Brown, V. Bulović, M.G. Bawendi, *Nat. Mater.* 13 (2014) 796.
- [8] U. Özgür, Y.I. Alivov, C. Liu, A. Teke, M.A. Reshchikov, S. Doğan, H. Morkoç, *J. Appl. Phys.* 98 (2005) 11.
- [9] S. Baruah, J. Dutta, *Sci. Technol. Adv. Mater.* 10 (2009) 013001.
- [10] A. Zaier, A. Meftah, A.Y. Jaber, A.A. Abdelaziz, M.S. Aida, *JKSUS.* 27 (2015) 356.
- [11] A. Chrissanthopoulos, S. Baskoutas, N. Bouropoulos, V. Dracopoulos, P. Pouloupoulos, S.N. Yannopoulos, *Photonics Nanostrut.* 9 (2011) 132.
- [12] G.J. Fodjouong, Y. Feng, M. Sangare, X. Huang, *Mat. Sci. Semicon. Proc.* 16 (2013) 652.
- [13] D. Yuvaraj, K.N. Rao, *Vacuum.* 82 (2008) 1274.
- [14] L. Feng, A. Liu, M. Liu, Y. Ma, J. Wei, B. Man, *Mater. Charact.* 61 (2010) 128.
- [15] T. Nguyen, N.T. Tuan, N.D. Cuong, N.D.T. Kien, P.T. Huy, V.H. Nguyen, D.H. Nguyen, *J. Lumin.* 156 (2014) 199.
- [16] R.K. Jamal, M.A. Hameed, K.A. Adem, *Mater. Lett.* 132 (2014) 31.
- [17] R. Mohamed, M.H. Mamat, A.S. Ismail, M.F. Malek, A.S. Zoolfakar, Z. Khusaimi, M. Rusop, *J. Mater. Sci. Mater. Electron.* 28 (2017) 16292.
- [18] Y.L. Lee, Y.S. Lo, *Adv. Funct. Mater.* 19 (2009) 604.
- [19] J.C. Hsiao, C.H. Chen, H.J. Yang, C.L. Wu, C.M. Fan, C.F. Huang, J.C. Hwang, *J. Taiwan Inst. Chem. Eng.* 44 (2013) 758.
- [20] H.J. Jeon, S.G. Lee, H. Kim, J.S. Park, *Appl. Surf. Sci.* 301 (2014) 358.
- [21] J. Ju, Y. Yamagata, T. Higuchi, *Adv. Mater.* 21 (2009) 4343.
- [22] A.P. Rambu, N. Iftimie, *Bull. Mater. Sci.* 37 (2014) 441.
- [23] Y. YU, K. Zhang, S. Sun, *Appl Surf. Sci.* 258 (2012) 7181.
- [24] K.S. Babu, A.R. Reddy, C. Sujatha, K.V. Reddy, A.N. Mallika, *J. Adv. Ceram.* 2 (2013) 260.
- [25] D.B. Barber, C.R. Pollock, L.L. Beecroft, C.K. Ober, *Opt. Lett.* 22 (1997) 1247.
- [26] S.K. Muzakir, Malaysia University Conference Engineering Technology 2014, Universiti Teknikal Malaysia Melaka, Malaysia, 2014.
- [27] K.S. Rathore, Deepika, D. Patidar, N.S. Saxena, K. Sharma, *AIP Conf. Proc.* 1249 (2010) 145.
- [28] S. Sönmezoğlu, R. Taş, S. Akın, M. Can, *Appl. Phys. Lett.* 101 (2012) 253301.